Measurement of Myocardial Blood Flow Using a Co-Injection Technique for Technetium-99m-Teboroxime, Technetium-96-Sestamibi and Thallium-201

Richard J. Di Rocco, William L. Rumsey, Bruce L. Kuczynski, Karen E. Linder, John P. Pirro, Rama K. Narra, and Adrian D. Nunn

The Bristol-Myers Squibb Pharmaceutical Research Institute, New Brunswick, New Jersey

We have compared apparent myocardial blood flow ($MBF_{apparent}$) indicated by ^{99m}Tc-teboroxime, ^{96}Tc-sestamibi and ^{201}Tl to true MBF indicated by radiolabeled microspheres using a technique for the co-injection of four radionuclides in the same animal. Studies were performed using rats in a single-pass model to obtain global MBF and using dogs in a multiple-pass model to determine regional MBF. To provide a wide range of MBF, adenosine was administered intravenously and the left anterior descending coronary artery was then ligated in the dogs, or hypercapnia was induced by decreasing respiratory frequency in the rats. The microsphere formula for determining MBF was applied to all agents. When $MBF_{apparent}$ was plotted as a function of true MBF, the ability of each agent to measure changes in true MBF was demonstrated by the proximity of the plotted function to the line of identity. For both the single and multiple-pass studies, statistical analysis of the nonlinear relationship between $MBF_{apparent}$ and true MBF showed that ^{201}Tl and ^{99m}Tc-teboroxime approximate true MBF better than ^{96}Tc-sestamibi ($p < 0.001$) under the conditions used in the present studies. In the single-pass studies, ^{99m}Tc-teboroxime approximated true MBF better than ^{201}Tl ($p < 0.05$), but in the multiple-pass experiments, ^{201}Tl approximated true MBF better than ^{99m}Tc-teboroxime in only one dog ($p < 0.01$) with no difference in the other two. Determination of the permeability-surface area product, PS, for each agent shows that the higher fidelity to true MBF obtained with ^{201}Tl and ^{99m}Tc-teboroxime is related to substantially greater PS values for these agents relative to ^{96}Tc-sestamibi.

J Nucl Med 1992; 33:1152–1159

It is well known that global or regional organ blood flow can be measured using radioactive microspheres in an indicator fractionation procedure, since microspheres are completely trapped and retained by the microvasculature (*1,2*). For soluble tracers such as thallium, sestamibi and teboroxime, however, neither the extraction nor the retention of the tracers by the myocardium is complete. If the microsphere flow equation is then applied to these agents and the resultant apparent value for myocardial blood flow ($MBF_{apparent}$) is plotted as a function of true MBF measured by co-injected microspheres, the plotted function will deviate from the line of identity in proportion to the net extraction of test agent by the target organ. The ability of the agent to indicate true flow is then clearly depicted by the proximity of the plotted function to the line of identity. Nevertheless, previous studies purporting to evaluate the sensitivity of SPECT MBF imaging agents to changes in MBF have used CPM/gram (*3*) or percent injected dose per gram (% ID/g) (*4*) as a function of MBF determined by co-injected radiolabeled microspheres. In those experiments, a linear correlation between the tissue radioactivity level and MBF, particularly at low flow levels, was interpreted as an indication of the efficacy of flow imaging by the agent. A linear correlation between the tissue radioactivity level and MBF is necessary but not sufficient for demonstrating the efficacy of a flow agent, since it is possible that an agent can have a high correlation coefficient for the linear relationship between tissue activity level and MBF, but underestimate true MBF determined from co-injected microspheres. For this reason, we believe it is more useful to use apparent MBF, calculated from tissue radioactivity levels arising from an agent, as the dependent variable to be plotted as a function of true flow determined from co-injected microspheres.

The purpose of the present investigation was to compare simultaneously the ability of thallium, sestamibi and teboroxime to measure both stimulated and ischemic MBF. The simultaneous comparison of MBF determined from four different agents, two of which are technetium compounds, can be accomplished by using ^{99m}Tc and ^{96}Tc to label teboroxime and sestamibi. This approach allows for a fair comparison of the agents and reduces the number of animals needed to make a comparison. Several methods

Received Sept. 26, 1991; revision accepted Jan. 31, 1992.

For reprints contact: Richard J. Di Rocco, The Bristol-Myers Squibb Pharmaceutical Research Institute, 1 Squibb Drive, P. O. Box 191, New Brunswick, NJ 08903-0191.

for the production of ^{96}Tc have been reported previously (*7,8,9,10*), and this isotope has been used to compare the long term behavior of the bone imaging agents Tc-HEDP and ^{186}Re-HEDP (*10*). However, the simultaneous use of compounds labeled with ^{99m}Tc and ^{96}Tc for the evaluation and comparison of technetium radiopharmaceuticals has not been previously reported.

METHODS

Determination of MBF from Single-Pass Extraction Studies in the Rat

Fifty-nine Sprague-Dawley rats (250–350 g) were used in these studies (n=13 for simultaneous evaluation and n=46 for separate evaluation). After induction of anesthesia (Nembutal, 50 mg/kg), femoral venous and arterial catheters were implanted and rats were then tracheotomized, thoracotomized, and artificially ventilated on room air using a small animal respirator (Harvard, Cambridge, MA). Arterial p_aCO_2 was set either at approximately 40 mm Hg (normocapnia) or about 60 mmHg (hypercapnia). Hypercapnia was used to increase MBF. Once the blood gas parameters were stabilized, a syringe pump (reference organ), set to withdraw blood at a rate of 1.15 ml/min, was connected to the femoral arterial catheter. With the pump on, the radionuclide injection mixture (see below) was rapidly (<0.5 sec) injected into the left ventricle via an apical puncture. For separate evaluation of agents in rats, a radiopharmaceutical agent was co-injected with ^{85}Sr-labeled microspheres, whereas for simultaneous evaluation of agents, all agents were co-injected with microspheres. Six seconds after injection the rat was decapitated and simultaneously, the syringe pump was stopped by a switch triggered by the guillotine. The heart was removed immediately, rinsed and weighed. For single-agent experiments, ^{85}Sr and ^{99m}Tc- or ^{201}Tl activities in the heart and arterial blood were counted using an LKB 1282 Compugamma gamma counter and the standard cross-over correction for ^{85}Sr and ^{99m}Tc or ^{201}Tl. Radionuclide counting and cross-over corrections used for multiple agent experiments, in which ^{85}Sr, ^{99m}Tc, ^{96}Tc and ^{201}Tl were co-injected, are described below.

Determinations of MBF from Multiple-Pass Studies in the Dog

Mongrel dogs (n=3, 15–17 kg) were anesthetized (I.V. Nembutal, 30 mg/kg). Both femoral arteries were cannulated for collection of blood (see below) and monitoring of arterial pressure using a transducer (Spectra Med Inc., Oxnard, Ca) interfaced with a polygraph (model 79D, Grass Instr., Quincy MA). A second pressure transducer (SPC-360, Millar Instr. Inc., Houston TX) was inserted into the left ventricle from the common carotid artery. The dogs were intubated with an endotracheal catheter, thoracotomized and respirated on room air to maintain P_aCO_2 at approximately 40 mmHg. For injection of radionuclides, a catheter was inserted in the left atrium. The left anterior descending coronary artery (LAD) was isolated and an electromagnetic flow probe (Carolina Medical Electronics, King, NC) was attached to it. A ligature was placed around the LAD just distal to the flow probe. Adenosine (160 μg/kg/min, dissolved in saline) was continuously infused via the femoral vein. After coronary flow reached a new steady state, the LAD was irreversibly ligated. Withdrawal of arterial blood using a syringe pump, set at 10 ml/min, was initiated. After approximately 30 sec elapsed, a 200 μl injection mixture of ^{99m}Tc-teboroxime, ^{96}Tc-sestamibi, ^{201}Tl, and ^{85}Sr-labeled microspheres was injected via the left atrial catheter. The catheter was then flushed rapidly (<5 sec) with 3 ml of physiological saline. Seventy seconds (1.17 min) from the start of the isotope injection, saturated KCl (10 ml) was rapidly injected into the atrial catheter to produce cardiac arrest. Collection of arterial blood was continued until cardiac arrest was evident by severe decreases in arterial and ventricular pressures. The heart was rapidly excised, placed in ice cold saline and rinsed free of blood. The heart was cut into 129 identifiable pieces each weighing between 1–2 g. The pieces were counted as described below.

Radiopharmaceutical Preparation

Technetium-99m-teboroxime was prepared as previously described (*11*). Thallium-201 was obtained from Dupont. The ^{96}Tc was produced by irradiation of natural molybdenum foil [$^{96}Mo(p,n)^{96}Tc$], in the 11 MeV cyclotron at the University of Wisconsin-Madison. Foils were irradiated for 2.5 hr at 15 μA, and stored for 4 days to allow the decay of the shorter-lived isotopes ^{94}Tc ($t_{1/2}$ = 4.88 hr) and ^{95}Tc (20 hr). Each foil of molybdenum metal, containing 55.5 to 148 mBq of ^{96}Tc, was dissolved by stirring and gentle heating in 6N HNO_3. After 1 hr, a white precipitate formed and the solution was deep red-brown. Neutralization (6N NH_4OH) followed by 4–6 drops of 30% H_2O_2 produced a clear red-brown solution. Further heating (10 min) and additional peroxide resulted in a clear, colorless solution. The resultant $^{96}TcO_4^-$ was extracted (77%–80% yield) by treatment with 3 × 5 ml of methyl ethyl ketone (MEK). The MEK was evaporated to dryness with N_2, and the $^{96}TcO_4$- redissolved in normal saline.

2-methoxyisobutylisonitrile (MIBI) was prepared as previously described (*12*). Technetium-96-sestamibi was prepared by adding 100 μl of ethanol, 50 μl 0.1N NaOH and 10 μl MIBI to 37-111 MBq $^{96}TcO_4^-$. This solution was reduced using 100 μl of sodium dithionite (50 mg/ml) in 0.1 *M* NaOH and heated at 100°C for 15 min. After cooling, the reaction mixture (RCP > 95%) was purified on PRP resin using a method described previously (*13*). The purified sample in ethanol was evaporated to dryness and redissolved in a 1/3 (v/v) ethanol/saline solution prior to injection. The final RCP was >99%, as determined by reversed phase HPLC (Nucleosil C-8 column 150×4.6 mm, Alltech Associates). Technetium-96$(MIBI)_6^+$ coeluted with authentic samples of $^{99}Tc(MIBI)_6^+$, prepared by a modification of the method of Abrams et al. (*14*). The radiochemical purity for all purified material was greater than 95% by HPLC.

Microsphere and Injectate Preparation

Strontium-85-labeled polystyrene microspheres (Dupont-NEN) in 1.0 ml 0.9% saline with 0.01% Tween-80 were used. The mean sphere size was 16.1±0.1 microns and the number of microspheres per vial (18.5 MBq/ml) was 15–18×10^6. Prior to mixing with a test compound, the vial of microspheres was vortexed briefly, then sonicated in a water bath for 15–20 min. For separate evaluation of agents in the single-pass studies, each 200-μl injection sample contained 0.093 MBq of ^{85}Sr (75–90×10^3 microspheres) and 0.093 MBq of ^{201}Tl or ^{99m}Tc. Assuming 5% fractional distribution of the cardiac output to rat heart and an average heart weight of approximately one gram, each rat heart received between 3,750 and 4,500 microspheres. For simultaneous evaluation of agents in the single-pass studies, each 200 μl injection sample contained between 0.093–0.13 MBq of each of the four radionuclides. In the dog experiments, we injected

2.3×10^6 microspheres per dog. Again assuming 5% fractional distribution of the cardiac output to myocardium, each dog heart received approximately 115×10^3 microspheres, yielding 1150 microspheres per gram at normal flows. In addition to the radiolabeled microspheres, each 1.3-ml injection sample for the dog experiments contained approximately 3.7 MBq of each of the other radionuclides.

Cross-Over Correction for Multiple-Agent Experiments

For each experiment, the radioactivity associated with each radionuclide in other radionuclide windows was determined using reference standards and the resultant crossover corrections were applied to tissue samples containing combined radionuclides. This was achieved by evaluating aliquots of the pure radionuclides individually and then combined for contribution of count rate in each counting window to determine the crossover contribution of each radionuclide in the other radionuclide windows. A summary of crossover contribution arising from the radioactivity associated with each radionuclide in other radionuclide windows is presented in Table 1. The reference radionuclide samples were prepared to approximate (±10%) the count rate of the respective radionuclides in the reference organ (blood). After counting the tissue samples in each of the radionuclide windows, the raw CPM were corrected for radioactive decay and crossover contribution of each isotope. The data were collected, evaluated, and processed using commercially available software (Microsoft Terminal and Excel®) for the IBM compatible personal computer.

Data Analysis

True MBF (ml/min/g), was calculated using:

$$\text{MBF (ml/min/g)} = \text{MBF}_{^{85}\text{Sr}} = \frac{\text{Syr. W.R.(ml/min)}(\text{CPM}_{^{85}\text{Sr}})_{\text{heart}}}{(\text{CPM}_{^{85}\text{Sr}})_{\text{blood}}(\text{heart wt. g})}, \quad \text{Eq. 1}$$

where Syr. W.R. is the syringe withdrawal rate. The ability of a test agent to approximate true flow was determined by substituting measured tissue and arterial blood counts arising from the agent, for ^{85}Sr counts in Equation 1. For both single- and multiple-pass experiments, the resulting apparent flow determination, $\text{MBF}_{\text{apparent}}$, is related to true flow determined from co-injected radiolabeled microspheres, $\text{MBF}_{^{85}\text{Sr}}$, by:

$$\text{MBF}_{\text{apparent}} = (\text{E})\ \text{MBF}, \quad \text{Eq. 2}$$

where E is the single-pass or net myocardial extraction of the agent. Since E varies between 0 and 1 $\text{MBF}_{\text{apparent}}$ will fall on the line of identity or below it when it is plotted as a function of MBF. Equation 2 can easily be solved to determine E at any given MBF by substituting the appropriate values for $\text{MBF}_{\text{apparent}}$ and MBF. In the single-pass model, E, MBF and capillary permeability-surface area product, PS, are related by the Crone-Renkin equation according to:

$$\text{E} = 1-e^{-(\text{PS/MBF})}, \quad \text{Eq. 3}$$

which can be transformed and rearranged to solve for PS:

$$\text{PS} = -\ln(1\text{-E})\text{MBF} \quad \text{Eq. 4}$$

For data from the rat single-pass experiments, we substituted values for E and MBF in Equation 4 to determine PS. PS was then plotted as a function of MBF and, using Systat™ software, a polynomial regression model was applied to the data to evaluate the significance of quadratic, linear and constant terms.

For single- and multiple-pass experiments, we derived a nonlinear expression for the regression of $\text{MBF}_{\text{apparent}}$ on MBF by substituting the Crone-Renkin expression for E, from Equation 3, in Equation 2:

$$\text{MBF}_{\text{apparent}} = \text{MBF}\ [1\text{-}e^{-(\text{PS/MBF})}] \quad \text{Eq. 5}$$

We then expressed the permeability-surface area product, PS, in Equation 5 as a linear function of MBF to get:

$$\text{MBF}_{\text{apparent}} = \text{MBF}\ \{1\text{-}e^{-[b+m(\text{MBF})]/\text{MBF}]}\} \quad \text{Eq. 6}$$

Values for b and m were determined using Systat™ software and Equation 6 as an exponential regression model to describe the relationship between $\text{MBF}_{\text{apparent}}$ and MBF in both the single- and multiple-pass experiments. In the rat single-pass studies, the significance of differences among the agents was assessed by analysis of covariance and, for the multiple-pass studies, the significance of differences among the parameters of the fit functions were evaluated using the t-test. We then substituted values for b and m, as well as high, normal and low values for MBF, into the Renkin-Crone expression for E between the brackets in Equation 6 to determine single-pass extraction for each agent in the rat.

RESULTS

The rat single-pass model was used to evaluate the effectiveness of the four-isotope cross-over correction by comparing data from the separate evaluation of the agents to data obtained from the simultaneous evaluation of the agents. In Figure 1, the data obtained from both simultaneous and separate determinations of $\text{MBF}_{\text{apparent}}$ are plotted as a function of true MBF for the three agents studied. For each of the agents the data sets were virtually superimposable. The similarity between the two sets of data

TABLE 1
Percent Crossover Contribution of Radionuclides Used in MBF Studies

Radionuclide/Window	^{201}Tl 60-100 keV	^{99m}Tc 120-155 keV	^{85}Sr 440-590 keV	^{96}Tc 650-860 keV
^{201}Tl	100	27.34 ± 0.67	0.36 ± 0.24	0.04 ± 0.03
^{99m}Tc	1.79 ± 0.04	100	0.07 ± 0.04	0.03 ± 0.03
^{85}Sr	10.63 ± 0.74	9.46 ± 0.37	100	0.39 ± 0.06
^{96}Tc	3.20 ± 0.18	3.61 ± 0.15	12.65 ± 0.24	100

Values represent the mean ± s.d. of five determinations.

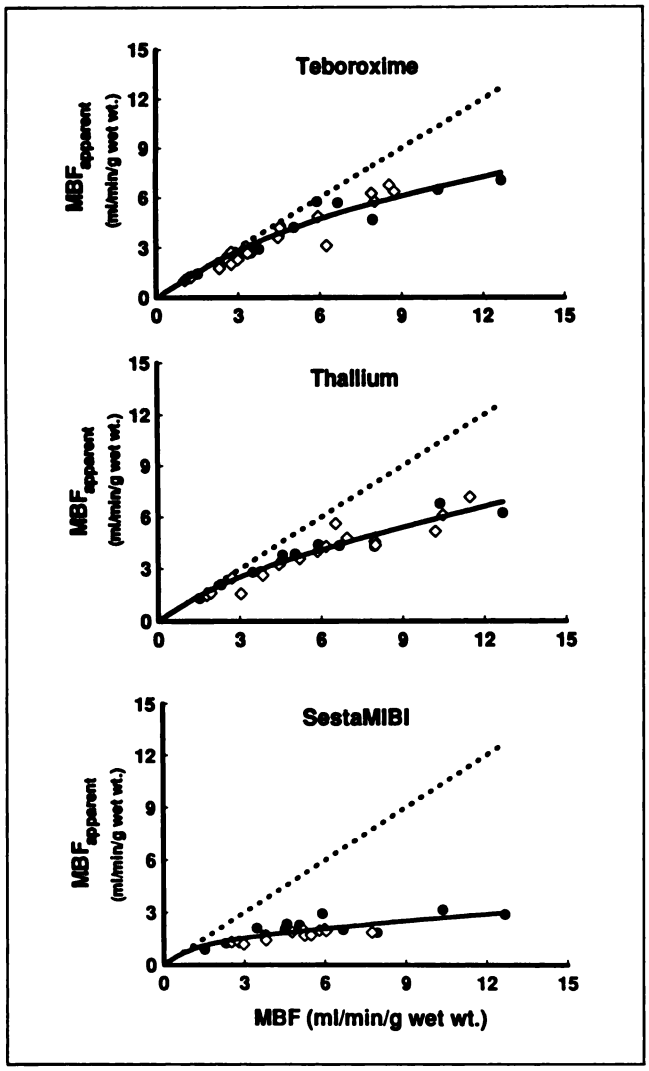

FIGURE 1. Scatter diagrams showing the relationship between $MBF_{apparent}$ and global MBF obtained in separate (◇) and simultaneous (●) evaluations of teboroxime, thallium and sestamibi in the rat single-pass model. The dashed line represents the line of identity. The fit functions for the nonlinear regressions are: $y = x[1-e^{-(7.22 + 0.33x)/x}]$ (teboroxime); $y = x[1-e^{-(4.20 + 0.45x)/x}]$ (thallium); $y = x[1-e^{-(1.76 + 0.127x)/x}]$ (sestamibi).

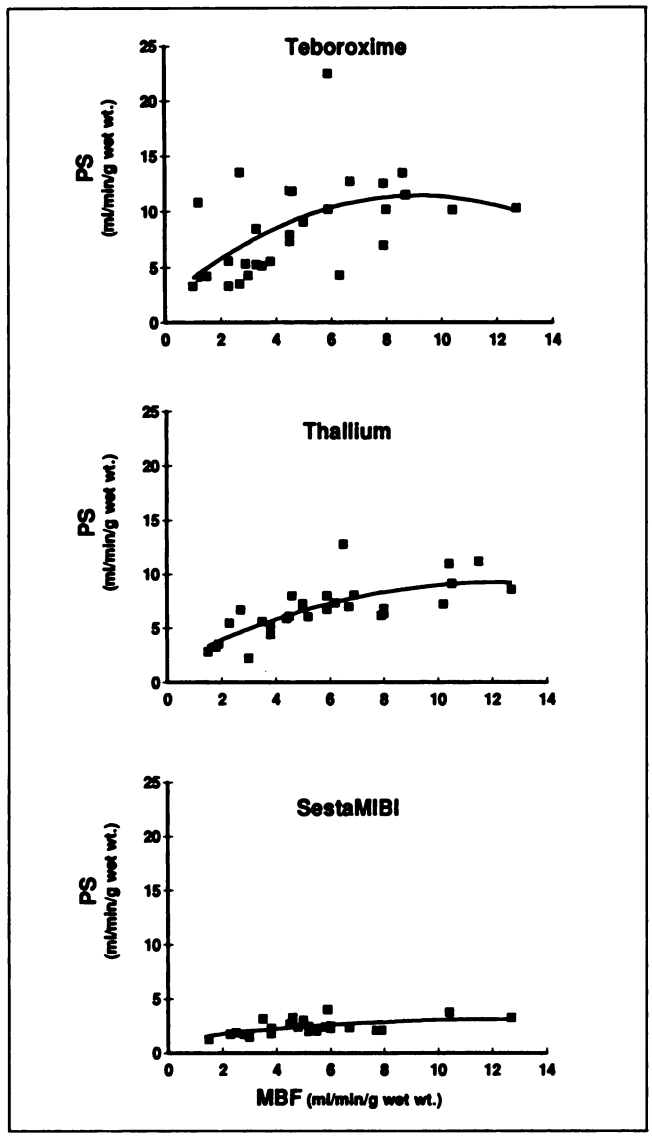

FIGURE 2. Scatter diagrams showing the relationship between calculated PS and true MBF obtained for each of the agents in the rat single-pass experiments. Fit functions obtained from polynomial regressions of PS on MBF were: $y = 2.152 + 2.024x - 0.11x^2$ (teboroxime); $y = 1.574 + 1.263x - 0.052x^2$ (thallium) and $y = 1.152 + 0.32x - 0.013x^2$ (sestamibi). See text for significance of quadratic, linear and constant terms.

indicates that the cross-over correction was accurate and that these data could be grouped together for the exponential regression analysis. The fit functions for the nonlinear regressions of $MBF_{apparent}$ on MBF are also shown in Figure 1. The nonlinear model for this regression analysis was derived after determining the nature of the function relating PS to MBF, as described below.

It was necessary to express PS as some function of MBF to reduce Equation 5 to a function of one variable, Equation 6, thereby obtaining a nonlinear model for the regression of $MBF_{apparent}$ on MBF. Values calculated for PS using Equation 4, from both separate and simultaneous evaluation of agents in the rat single-pass studies, were pooled and are shown as a function of MBF, together with quadratic fit functions, in Figure 2. The polynomial regression analysis for the relationship between PS and MBF revealed significant linear terms for teboroxime ($p < .03$) and thallium ($p < .01$), whereas the constant and quadratic terms for these compounds were not significant. For sestamibi, on the other hand, only the constant term was significant ($p < .05$). In no case was the quadratic term significant. We therefore used a linear expression for PS in the Crone-Renkin equation to derive Equation 6, which was used for the nonlinear regression of $MBF_{apparent}$ on MBF shown in Figure 1. We substituted a linear expression for PS, instead of its exact value, -MBF[ln(1-E)], because substitution of the latter would yield Equation 2 upon simplification. This does not reduce Equation 5 to a func-

tion of one variable, since E is not constant with respect to flow.

A composite of the fit functions for the relationship between $MBF_{apparent}$ and true MBF is shown in Figure 3 to facilitate comparison of the three agents. For all compounds, the deviation of the respective fit functions from the line of identity increases exponentially as true MBF increases, but ^{99m}Tc-teboroxime and ^{201}Tl more closely approximate true flow than ^{99m}Tc-sestamibi. For example, at a normal rat MBF level of 5.0 ml/min/g, $MBF_{apparent}$ is 4.15 ml/min/g and PS is 8.87 ml/min/g for ^{99m}Tc-teboroxime. For ^{201}Tl, $MBF_{apparent}$ is 3.62 ml/min/g and PS is 6.45 ml/min/g. On the other hand, for ^{99m}Tc-sestamibi, $MBF_{apparent}$ is only 1.9 ml/min/g with a correspondingly low PS value of 2.4 ml/min/g. Analysis of covariance revealed that the difference between thallium and teboroxime was significant ($p < 0.05$), and sestamibi was different from both teboroxime and thallium ($p < 0.001$). Estimated values for single-pass extraction, E, of each of the agents at low, normal and high MBF levels are shown in Table 2.

Having validated the cross-over correction and justified our nonlinear regression model for the relationship between $MBF_{apparent}$ and MBF, we proceeded to examine the agents simultaneously in the dog model where it was possible to obtain information concerning a full range of regional MBF's using both LAD occlusion and adenosine stimulation in a multiple-pass paradigm. Average arterial blood gasses and pH just before the adenosine infusions in the dogs were in the normal range: 77.4 (p_aO_2); 37.9 (p_aCO_2) and 7.35 (pH). Coronary flow and measures of cardiac performance are presented in Table 3, which clearly shows that intravenous adenosine increased coronary blood flow and reduced systolic and diastolic blood pressure by 21% and 31%, respectively. Figure 4 shows, for each dog, $MBF_{apparent}$ as a function of MBF for each of the agents in dissected myocardial sections. The variable response to adenosine is evident from the variation in the maximum flows depicted on the abscissa. As shown in Figures 1 and 3 for the single-pass model, Figure 4 shows, in a multiple-pass model, that teboroxime and thallium more closely approximate the line of identity than sestamibi. The difference for the parameters of the fit functions

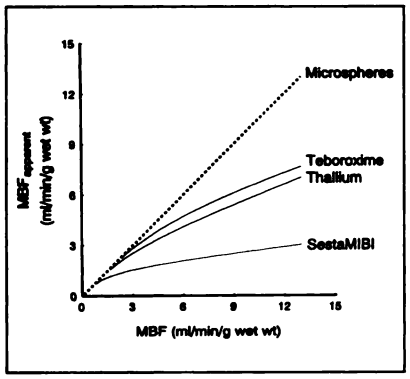

FIGURE 3. Composite of the fit functions shown in Figure 1 for the relationship between $MBF_{apparent}$ and true MBF from separate and simultaneous evaluations of agents in the rat single-pass experiments.

TABLE 2
Single-pass extraction values for each of the agents at low, middle and high MBF levels shown

MBF (ml/min/g)	Thallium	Teboroxime	Sestamibi
1.0	1.00	1.00	1.00
5.0	0.72	0.83	0.38
12.0	0.55	0.61	0.24

Values for E were calculated by substituting the indicated values for MBF into the expression in the brackets of the following regression equations for the data shown in Figure 1: $MBF_{apparent} = MBF[1-e^{-(7.22 + 0.33\ MBF)/MBF}]$ (teboroxime); $MBF_{apparent} = MBF[1-e^{-(4.20 + 0.45\ MBF)/MBF}]$ (thallium); $MBF_{apparent} = MBF[1-e^{-(1.76 + 0.127\ MBF)/MBF}]$ (sestamibi).

for thallium and teboroxime was significant for only one dog ($p < 0.01$) and both ^{201}Tl and teboroxime were different from sestamibi in all dogs ($p < 0.001$).

DISCUSSION

By using a method that requires the left ventricular injection of a mixture of radiolabeled microspheres and one or more test agents simultaneously (*6*), we were able to determine global myocardial blood flow (MBF) in a single-pass model in the rat. We also used a multiple-pass model, with a 70 sec circulation time, to determine regional MBF in dogs with focal myocardial ischemia and adenosine-stimulated blood flow. We were thus able to compare simultaneously the sensitivity of these agents to changes in regional MBF over a spectrum of flows encompassing ischemia and stress simply by determining the tissue and blood levels of activity arising from each of the agents using the gamma counter. The obvious advantage of this approach is that it provides a more accurate comparison than is possible when different agents are tested in different animals, or when gamma counter counts are compared to tomographic counts. These studies demonstrate, as shown in Figure 1, that it is possible to use two technetium isotopes to evaluate two technetium-labeled radiopharmaceuticals simultaneously in the same animal without loss of accuracy. This is important because it can reduce inter-animal sources of variation and permits the use of fewer animals. In addition, it is clear from Figures 3 and 4 that when $MBF_{apparent}$ is plotted as a function of true MBF, the fidelity of flow imaging by the agent is unambiguously indicated by the proximity of the plotted function to the line of identity. This representation pro-

TABLE 3
Effect of Adenosine Infusion on Coronary Blood Flow, Blood Pressure and Heart Rate

	Coronary flow (ml/min)	Systolic pressure (mmHg)	Diastolic pressure (mmHg)	Heart rate (bpm)
Pre-adenosine	26 ± 1	132 ± 10	112 ± 9	160 ± 11
Adenosine	52 ± 7	104 ± 11	77 ± 5	172 ± 17

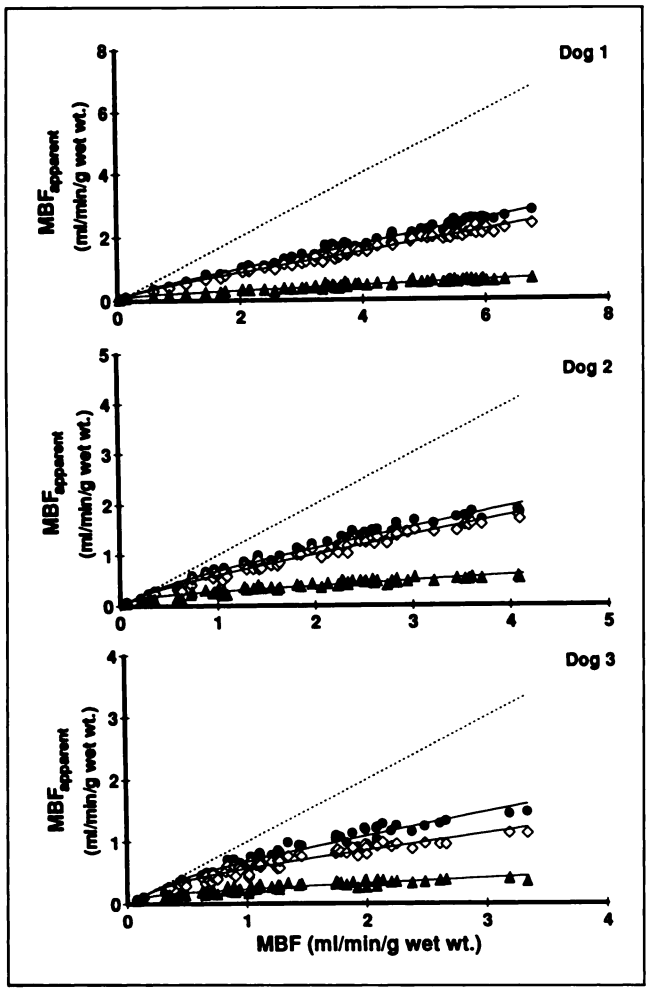

FIGURE 4. Scatter diagram for the relationship between $MBF_{apparent}$ and true MBF in pieces of dog myocardium after left atrial injection of a mixture of ^{85}Sr-labeled microspheres, ^{99m}Tc-teboroxime: ◇, ^{96}Tc-sestamibi: ▲ and ^{201}Tl: ●. $MBF_{apparent} = MBF[1-e^{-(b + m*MBF)/MBF}]$ was used as the regression model as described in the text. The dashed line represents the line of identity. Equations for each of the dogs were: Dog 1: $y = x[1-e^{-(0.39 + 0.49x)/x}]$ (thallium); $y = x[1-e^{-(0.33 + 0.40x)/x}]$ (teboroxime); $y = x[1-e^{-(0.17 + 0.08x)/x}]$ (sestamibi); Dog 2: $y = x[1-e^{-(0.65 + 0.51x)/x}]$ (thallium); $y = x[1-e^{-(0.45 + 0.48x)/x}]$ (teboroxime); $y = x[1-e^{-(0.22 + 0.11x)/x}]$ (sestamibi); Dog 3: $y = x[1-e^{-(0.14 \pm 1.46x)/x}]$ (thallium); $y = x[1-e^{-(0.22 + 0.96x)/x}]$ (teboroxime); $y = x[1-e^{-(0.15 + 0.43x)/x}]$ (sestamibi).

vides an accurate method for the comparison of different agents that is not possible when tissue radioactivity levels are plotted as a function of myocardial blood flow. While a strong linear relationship between tissue activity level and true MBF is a necessary requirement of a good flow indicator, it is not sufficient. In addition, a true flow indicator must by definition have the same ratio of heart to reference organ activity as coinjected radiolabeled microspheres. Thus, a high correlation between tissue radioactivity and true MBF is not an indication of high fidelity flow imaging by an agent, since the apparent flow indicated by tissue radioactivity can still underestimate true flow considerably. Ambiguities arise from a failure to compare $MBF_{apparent}$ to true MBF. For example, when CPM per gram is plotted as a function of true MBF, it is difficult to compare the relative efficacies of different compounds, since tissue activity level will then depend not only on the net myocardial extraction of the agent, but also the injected dose. Percent injected dose can be used as the dependent variable to facilitate comparison of different agents, however this approach still gives no information concerning the accuracy of flow imaging by the agent for the reasons just described. Figures 3 and 4 show that ^{201}Tl and ^{99m}Tc-teboroxime more closely approximate the line of identity than ^{96}Tc-sestamibi, thereby indicating that they are more sensitive to changes in MBF under these conditions owing to their higher single-pass or net myocardial extractions. This conclusion follows from Equation 2, which shows that E increases as the ratio ($MBF_{apparent}$/MBF) increases, and is supported by the estimated values for E shown in Table 2.

We used Equation 2 as the basis for deriving Equation 6 for the nonlinear regression of $MBF_{apparent}$ on true MBF in the case of both single- and multiple-pass experiments. This is warranted because, for thallium and sestamibi, the clearance from the heart over the 70 sec multiple-pass interval is negligible and, for these agents, E is virtually identical to E_{Net}. For teboroxime E_{Net} can be shown to be a constant fraction of E. When E is replaced by E_{net} at time t (t = net extraction interval in the dog studies = 70 sec = 1.17 min) to yield:

$$MBF_{apparent} = (E_{Net})\ MBF, \qquad \text{Eq. 7}$$

we can calculate an approximate value for E_{Net} according to:

$$E_{Net} = E(e^{-kt}), \qquad \text{Eq. 8}$$

where k is the efflux rate constant and t is time in minutes. We have found (*11*) that the clearance of teboroxime from the dog heart is described by a bi-exponential function of the type:

$$\text{Heart (\%ID)} = A(e^{-0.194t}) + B(e^{-0.0069t}). \qquad \text{Eq. 9}$$

For t = 1.17 min, only the first exponential term is significant and, therefore, E_{Net} for teboroxime will be:

$$E_{Net} = E(e^{-0.194*1.17}) = (E)0.80. \qquad \text{Eq. 10}$$

Since E_{Net} is either equal to E or is a constant fraction of E, Equation 6 could be used as the nonlinear regression model for both the single- and multiple-pass experiments. The greater extractions of teboroxime and thallium relative to sestamibi, are consistent with the higher values for the cofactors of the fit functions describing the relationship between PS and MBF for these agents, as shown in Figure 2. The significance of the constant term in the polynomial regression of PS on MBF for sestamibi explains the relative insensitivity of this agent to change in MBF shown in Figures 3 and 4.

Our derivation of a nonlinear regression model to de-

scribe the relationship between $MBF_{apparent}$ and true MBF relies upon the Renkin-Crone model, and its theoretical assumptions. It is clear that Equation 3 applies to all flow levels, owing to the presence of a flow term and that simultaneous measurement of $MBF_{apparent}$ and true MBF effectively measures E for any set of conditions within the piece of tissue sampled. On the other hand, the model does not account for potential differences in the extraction mechanisms of different agents under diverse conditions, such as the numerous factors arising during ischemia. Despite this limitation, the Renkin-Crone equation can be incorporated into a nonlinear regression for the relationship between $MBF_{apparent}$ and true MBF because goodness of fit does not require that a model provide a total mechanistic explanation of the underlying phenomenon. In any case, our findings are consistent with previous reports demonstrating a greater uptake of teboroxime relative to sestamibi in cultured rat and chick myocytes, where there is no flow component (*15,16*). Studies in isolated perfused rabbit hearts have demonstrated a greater uptake of teboroxime and thallium relative to sestamibi (*5,17*). On the other hand, whereas Leppo and Meerdink (*5*) found that the extraction of teboroxime was greater than that of thallium, Marshall et al. (*18*) found the opposite. Our finding of greater net extraction of thallium relative to teboroxime in the dog studies is the opposite of the order observed in our single-pass experiments. This may be attributed to species differences in extraction, or a greater rate of teboroxime washout relative to thallium. In any case, a comparison of a number of extraction studies shows that, notwithstanding some variability among results, teboroxime extraction approximates that of thallium and the extraction of both is greater than that of sestamibi (*19*). The reported marginal differences between the extractions of teboroxime and thallium may have little impact on clinical imaging.

It is well-known that teboroxime washes out of the human heart with a half-time of about ten minutes (20, 21), whereas the washout of sestamibi from the heart is much slower, declining to around 80% of the peak initial value by three hours after injection (*22*). Accordingly, it is desirable to acquire teboroxime SPECT images rapidly after injection (*23*), but sestamibi images are typically obtained after 1 hr to minimize background activity (*22*). In the present multiple-pass experiments, the agents were co-injected with radiolabeled microspheres and arterial blood was collected for 70 sec to allow the microspheres to clear the circulation. Since teboroxime image acquisition time exceeds 70 sec the full affect of washout during image acquisition is not represented in the present results. Thus, despite the differences between teboroxime and sestamibi observed in the present studies, the current overall clinical sensitivity and specificity of both agents are comparable to that of thallium (*19,21,22,24*). This implies that the net extraction of the agents is comparable over the intervals between injection and completion of image acquisition in current imaging protocols. Nevertheless, since fewer patients have been studied with teboroxime, it is expected that improvements in image acquisition and interpretation (*25*) will make better use of teboroxime's high extraction and, consequently, its ability to indicate true MBF with high fidelity. This should lead to an improvement in specificity and sensitivity.

One benefit of the washout characteristic of teboroxime is that repeat studies, yielding images comparable to those obtained with ^{201}Tl, can be performed within a few hours of each other (*21*). Another benefit to be explored is the additional information contained in the regional washout profile of teboroxime (*19*). An increase in the accuracy of diagnosing ischemia at stress could arise from reversal, with time, of the ratio of ischemic to nonischemic tissue activity levels that results from differential washout of teboroxime from high and low flow regions (*20*). In addition, the qualitative basis of present diagnostic decisions may be superseded by quantitative determination of MBF from a knowledge of regional washout rates and the blood to tissue partition coefficient for teboroxime.

ACKNOWLEDGMENTS

The authors thank Mrs. L. Belnavis and Ms. C. Hood for their excellent technical assistance and Professor R. Jerry Nickles from the University of Wisconsin-Madison Medical School for preparing the samples of ^{96}Tc metal used in this study.

REFERENCES

1. Dole WP, Jackson DL, Rosenblatt JI, Thompson WL. Relative error and variability in blood flow with radiolabeled microspheres. *Am J Physiol* 1982;243:H371–H378.
2. Nose Y, Nakamura T, Nakamura M. The microsphere method facilitates statistical assessment of regional blood flow. *Basic Res Cardiol* 1985;80: 417–429.
3. Nielson AP, Morris KG, Murdock R, Bruno FP, Cobb FR. Linear relationship between the distribution of thallium-201 and blood flow in ischemic and nonischemic myocardium during exercise. *Circulation* 1980; 61:797–801.
4. Mousa SA, Cooney JM, Williams SJ. Relationship between regional myocardial blood flow and the distribution of ^{99m}Tc-sestamibi in the presence of total coronary artery occlusion. *Am Heart J* 1990;119:842–847.
5. Leppo JA, Meerdink DJ. Comparative myocardial extraction of two technetium-labeled BATO derivatives (SQ 30217, SQ 32014) and thallium. *J Nucl Med* 1990;31:67–74.
6. Irwin GH and Preskorn SH. A dual label radiotracer technique for the simultaneous measurement of cerebral blood flow and the single-transit cerebral extraction of diffusion-limited compounds in the rat. *Brain Res* 1982;249:23–30.
7. Edwards JE, Pool ML. Radioactive Isotopes of Mo and Tc. *Phys Rev* 1947; 72:384–389.
8. Monaro S, Barrette J, Boutard A. Energy levels of ^{96}Mo excited in the decay of the $^{96m,g}Tc$ isomeric pair and ^{96}Nb. *Can J Phys* 1968;46: 2375–2397.
9. Cesareo R, Frevert L, Flammersfeld A. Decay of ^{96}Tcg and ^{96}Tcm. *Zeit Phys* 1967;205:174–180.
10. Mausner LF, Kurczak S, Srivastava SC. Production of ^{96}Tc, a long-lived substitute for ^{99m}Tc. Proc. 8th Int. Conf. on Radiopharmaceutical Chemistry 1990. Princeton, NJ. pp. 1–3.
11. Narra RK, Nunn AD, Kucynski BL, Feld T, Wedeking P, Eckelman WC. A neutral technetium-99m complex for myocardial imaging. *J Nucl Med* 1989;30:1830–1837.
12. Ramalingam K. Process for preparing 2-methoxyisobutylisonitrile. US Patent 4,864,051, Sept. 5, 1989.
13. Jurisson SS, Hirth W, Linder KE, et al. Chloro→Hydroxy substitution on

technetium BATO (TcCl(Dioxime)$_3$BR) complexes. *Nucl Med Biol* 1991;18:735–744.
14. Abrams MJ, Davison A, Jones AG, et al. Synthesis and characterization of hexakis (alkyl isocyanide) and hexakis (aryl isocyanide) complexes of technetium(I). *Inorg Chem* 1983;22:2798–2800.
15. Maublant JC, Moins N, Gachon P. Uptake and release of two new Tc-99m labeled myocardial blood flow imaging agents in cultured cardiac cells. *Eur J Nucl Med* 1989;15:180–182.
16. Kronauge JF, Chiu ML, Cone JS, et al. Comparison of neutral and cationic myocardial perfusion agents: characteristics of accumulation in cultured cells. *Nucl Med Biol* 1992;19:141–148.
17. Leppo JA, Meerdink DJ. Comparison of the myocardial uptake of technetium-labeled isonitrile analogue and thallium. *Circ Res.* 1989;65: 632–639.
18. Marshall RC, Leidholdt EM, Zhang D-Y, et al. The effect of flow on the technetium-99m-teboroxime (SQ30217) and thallium-201 extraction and retention in rabbit heart. *J Nucl Med* 1991;32:1979–1988.
19. Nunn, AD. Is there additional useful information in the myocardial washout characteristics of teboroxime. *J Nucl Med* 1991,32:1988–1991.
20. Stewart RE, Schwaiger M, Hutchins GD, et al. Myocardial clearance kinetics of technetium-99m-SQ 30217: a marker of regional myocardial blood flow. *J Nucl Med* 1990;31:1183–1190.
21. Seldin DW, Johnson LL, Blood DK, et al. Myocardial perfusion imaging with technetium-99m-SQ 30217: comparison with thallium-201 and coronary anatomy. *J Nucl Med* 1989;30:312–319.
22. Wackers FJTh, Berman DS, Maddahi J, et al. Technetium-99m hexakis 2-methoxyisobutyl isonitrile: human biodistribution, dosimetry, safety and preliminary comparison to thallium-201 for myocardial perfusion imaging. *J Nucl Med* 1989;30:301–311.
23. Iskandrian AS, Heo J, Nguyen T, Mercuro J. Myocardial imaging with Tc-Teboroxime: technique and initial results. *Am Heart J* 1991;121:889–94.
24. Fleming RM, Kirkeeide RL, Taegtmeyer H, et al. Comparison of technetium-99m teboroxime tomography with automated quantitative coronary arteriography and thallium-201 tomographic imaging. *J Am Coll Cardiol* 1991;17:1297–1302.
25. Burns RJ, Wright L. Three-minute acquisition of exercise Tc-99m teboroxime cardiac SPECT with a single-head camera detector [Abstract]. *J Nucl Med* 1991;32:929.

(continued from page 5A)

FIRST IMPRESSIONS

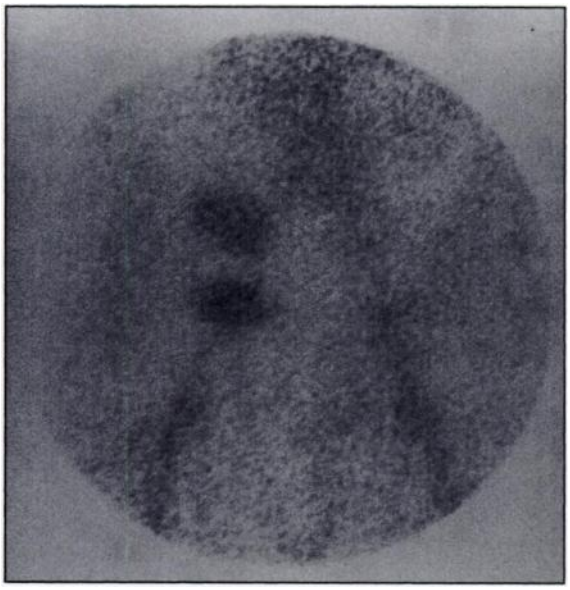

R 2 min L

PURPOSE
Evaluation of renal perfusion and function 24 hr after transplantation was performed. This 19-yr-old patient received an en bloc pediatric cadaveric transplant from a 3-yr-old donor. Both transplants are perfused and functioning adequately.

TRACER
10 mCi (370 MBq) of ^{99m}Tc-DTPA

ROUTE OF ADMINISTRATION
Intravenous injection

TIME AFTER INJECTION
2 min

INSTRUMENTATION
Siemens Orbiter LFOV gamma camera with a LEAP collimator

CONTRIBUTORS
H.R. Balon, MD and C.E. Nagle, MD

INSTITUTION
Nuclear Medicine Department, William Beaumont Hospital, Royal Oak, Michigan